

## **SIR-Spheres<sup>®</sup> activity measurements reveal systematic miscalibration**

Stephen A. Graves<sup>1,2,3</sup>, Molly Martin<sup>1</sup>, Ashok Tiwari<sup>1,4</sup>, Michael Merrick<sup>1,2</sup>, John Sunderland<sup>1,4</sup>

<sup>1</sup> Department of Radiology, University of Iowa, 3883 JPP, 200 Hawkins Dr., Iowa City, IA 52242, USA

<sup>2</sup> Department of Biomedical Engineering, University of Iowa, 5601 Seamans Center, Iowa City, IA 52242, USA

<sup>3</sup> Department of Radiation Oncology, University of Iowa, LL-W PFP, 200 Hawkins Dr., Iowa City, IA 52242, USA

<sup>4</sup> Department of Physics, University of Iowa, 203 Van Allen Hall, Iowa City, IA 52242, USA

### **Corresponding author:**

Stephen A. Graves, PhD, DABR

Department of Radiology

University of Iowa

200 Hawkins Dr., Iowa City, IA 52242, USA

Phone: +1-319-678-7986

Fax: +1-319-356-2220

ORCID: 0000-0003-2732-3064

Email: stephen-a-graves@uiowa.edu

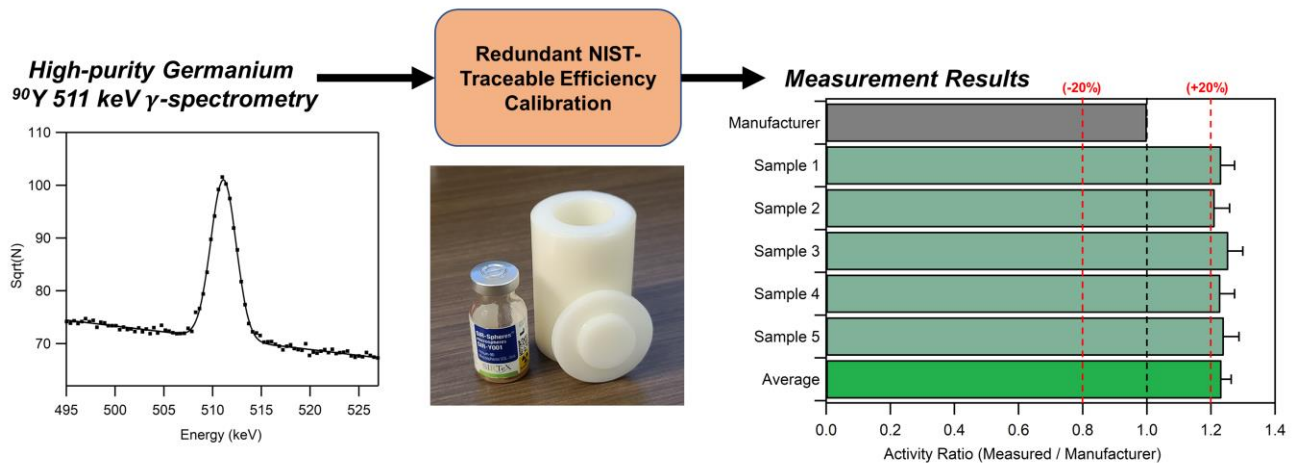
**Keywords:** TARE, radioembolization, radiopharmaceutical therapy

**Running title:** SIR-Spheres<sup>®</sup> activity miscalibration

## ABSTRACT

The purpose of this work was to perform an independent and National Institute of Standards and Technology (NIST)-traceable activity measurement of  $^{90}\text{Y}$  SIR-Spheres<sup>®</sup>. Gamma spectroscopic measurements of the  $^{90}\text{Y}$  internal pair production decay mode were made using a high-purity germanium detector. Measured annihilation radiation detection rates were corrected for radioactive decay during acquisition, dead time, source attenuation, and source geometry effects. Detection efficiency was determined by two independent and NIST-traceable methods. Measured SIR-Sphere<sup>®</sup> vials (n=5) were found to contain more activity than specified by the manufacturer calibration – on average the ratio of measured activity to calibrated was  $1.233 \pm 0.030$ . Activity measurements made using two distinct efficiency calibration methods were found to agree within 1%. Therefore, the primary SIR-Spheres<sup>®</sup> activity calibration appears to be a significant underestimate of true activity.

### SIR-Spheres<sup>®</sup> activity measurements reveal systematic miscalibration



## INTRODUCTION

Dosimetry-guided radiopharmaceutical therapy is gaining traction in nuclear medicine and adjacent fields. Several agents have been approved with a requirement of dosimetry ( $^{131}\text{I}$ -MIBG,  $^{90}\text{Y}$  Theraspheres<sup>®</sup>), but even agents that do not currently carry a dosimetry mandate (e.g.  $^{177}\text{Lu}$ -DOTATATE,  $^{90}\text{Y}$  SIR-Spheres<sup>®</sup>) are increasingly being used under dosimetry-guided treatment paradigms. This is evidenced by a recent survey indicating that a majority (64%) were clinically administering SIR-Spheres<sup>®</sup> according to absorbed dose rather than body surface area-derived activity, which is the current U.S. Food and Drug Administration approved label method (*1*). Additionally, combination therapy approaches have been gaining popularity, particularly in combining radiopharmaceutical therapy with external beam radiotherapy, immunotherapy, or both (*2-5*). As this trend continues, it is critical that our field develops standard practices for measurement, delivery, and verification of radiation absorbed dose. Perhaps the most fundamental consideration is whether we are administering a quantity of radioactive material that is consistent with what is prescribed by the authorized user.

In this work we describe a series of two independent high purity germanium (HPGe) spectrographic measurements – grounded to National Institute of Standards and Technology (NIST)-traceable sources and measurement – to determine the activity contained within SIR-Spheres<sup>®</sup> vials prior to patient treatment in relation to the manufacturer-provided activity calibration.

## MATERIALS AND METHODS

### SIR-Spheres<sup>®</sup> and Manufacturer Calibration

$^{90}\text{Y}$  SIR-Spheres<sup>®</sup> are received from the manufacturer (Sirtex Medical Limited; Woburn, MA) in a glass vial contained within a lead pig. With agitation spheres are uniformly suspended in ~5 mL of sterile water, however within ~2 minutes of non-agitation the microspheres settle to the bottom of the vial, with approximately 4 mL of water supernatant. Vials can be received from the manufacturer with varying activity levels, by way of delivery on various days prior to the date and time of reference calibration, however the same number of spheres (+/-5%) is present within a vial regardless of the activity provided. Each vial is specified by the manufacturer to contain 3 GBq (81 mCi)  $\pm$  10% at the date and time of calibration (often the day of treatment at 18:00 EST). Vials expire 24 hours following the calibration date and time, regardless of the pre-calibration date of receipt.

Although the nominal activity of any individual vial is specified as 3 GBq  $\pm$  10%, upon request the manufacturer will provide a certificate of measurement of the vial at the production facility. This certificate contains an exact activity measurement of a particular vial within the manufacturer's own ion chamber, decay corrected to the date/time of calibration. Activity within this report is provided with four significant figures (e.g. 3.004 GBq) and without any associated measurement uncertainty specification. This certificate, and the associated

activity vial, is the primary mechanism by which a user site or radiopharmacy establishes dose calibrator dial settings prior to initiation of a clinical program. This procedure was performed at the University of Iowa in 2012 for initial dose calibrator configuration. An additional certificate was obtained for one of the samples measured in this work (received April 26, 2021) to confirm that the University of Iowa dose calibrator remained traceable to the manufacturer's ion chamber. A single dose calibrator (Capintec CRC-15R) was used for all measurements described herein.

### HPGe Spectrometry

Yttrium-90 activity measurements were performed by HPGe spectroscopic measurements (Ortec GEM20P4-70) via counting of the 511 keV annihilation emission produced following the 32 parts-per-million internal pair production decay mode of  $^{90}\text{Y}$  (6). Energy and peak-shape calibration was performed using NIST-traceable sources ( $^{241}\text{Am}$ ,  $^{57}\text{Co}$ ,  $^{137}\text{Cs}$ ,  $^{60}\text{Co}$ , and  $^{152}\text{Eu}$ ;  $\sigma=1.16\%$ ; Eckert & Ziegler). A custom high-density polyethylene (HDPE) source holder (1 cm thick,  $\rho = 0.966 \pm 0.009 \text{ g/cm}^3$ ) was manufactured and utilized to assure local positron annihilation during spectral acquisition. This source holder and an example patient vial are shown in Figure 1.

All patient vials were measured at a distance of 210 cm from the detector (surface to surface distance), with acquisition durations of 3 – 6 hours. All samples were measured one day prior to the calibration date, and thus were expected to be in the range of 4 – 5 GBq. Despite the lack of abundant gamma emissions, the high levels of activity and associated Bremsstrahlung emissions induced relatively high dead times during data collection – ranging between 22.5% and 25.6% depending on the sample, as estimated by Ortec HPGe electronics. Due to the importance of dead time correction in these measurements, a separate experiment was performed to validate the accuracy of dead time estimation provided by the ORTEC electronics. Details regarding this measurement are included in the Supplemental Section. Spectral peak areas were determined using the SAMPO algorithm, which employs a well-established peak-fitting method (7).



**Figure 1.** Custom high-density polyethylene source holder, and example SIR Sphere patient vial.

## Efficiency Calibration

Detector efficiency calibration was performed via two distinct methods, described below.

- *Method 1:* NIST-traceable sources ( $^{241}\text{Am}$ ,  $^{57}\text{Co}$ ,  $^{137}\text{Cs}$ ,  $^{60}\text{Co}$ , and  $^{152}\text{Eu}$ ; Eckert & Ziegler) were used to establish absolute detection efficiency as a function of energy, with the sources positioned at the same position as the patient vial during counting. This efficiency estimate does not account for self-attenuation of 511 keV emissions within the source vial and holder, so Monte Carlo simulations were performed to determine the appropriate self-absorption correction factor. Simulations were performed in MCNP v6.2, and verification was performed using the Geant4 Application for Tomographic Emission (GATE). Details regarding these simulations are provided in the Supplemental Material.
- *Method 2:* A NIST-traceable calibrated quantity of  $^{18}\text{F}$  (~37 MBq in 3 mL) was placed within an empty SIR Spheres® vial, and spectral acquisition was performed under identical conditions to what was performed for  $^{90}\text{Y}$  measurements, including geometry and dead time. Under these conditions, a 511 keV efficiency calibration was obtained by comparing the observed 511 keV count rate to the known emission rate within the  $^{18}\text{F}$  sample. Fluorine-18 sample calibration was performed by use of a  $^{68}\text{Ge}/^{68}\text{Ga}$  standard tied to a NIST  $^{18}\text{F}$  measurement for dose calibrator configuration (8). Assay of the  $^{18}\text{F}$  sample was performed under calibrated conditions (3 mL in a 5 mL syringe) with quantitative transfer and decay correction prior to spectrometry.

## Activity Determination and Measurement Uncertainty

Yttrium-90 activity was determined from the measured peak area, detector live-time, detection efficiency, and literature value of the internal pair production branching ratio (6). The branching ratio measured by R. Selwyn –  $(31.86 \pm 0.47) \times 10^{-6}$  – was utilized for this work, which generally agrees with other measurements (9), as well as being the value recommended by the Decay Data Evaluation Project, last updated in 2015 (10). Second-order corrections were applied for radioactive decay during spectral acquisitions, background 511 keV count rate, and geometry effects ( $^{18}\text{F}$  vs.  $^{90}\text{Y}$ ). These corrections are detailed in the Supplemental Material.

Determination of measurement uncertainty in this work follows NIST Technical Note 1297 (11) and the International Organization for Standardization (ISO) Expression of Uncertainty (12). Type A uncertainty in this experiment consisted of statistical uncertainty in measured 511 keV peak area for each sample. Several sources of Type B uncertainty were characterized, including Monte Carlo statistical uncertainty, glass vial thickness (inter- and intra-vial variability), source holder thickness, positron range effects, dead time correction precision, positron branching ratio uncertainty, and several additional factors relating to detection efficiency determination. All uncertainties are specified in terms of standard error ( $1\sigma$ ), and propagation followed the standard “root-sum-of-squares” method (13).

## RESULTS

The local dose calibrator at the University of Iowa was found to agree with the manufacturer's certificate of calibration within 0.5%, suggesting that historic dose calibrator readings (Capintec CRC-15R; dial setting #56x10) have been a reasonable surrogate for the manufacturer's activity calibration. A review of the last 100 patient vials received by the University of Iowa reveals that the manufacturer has been consistent with their product label of 3.00 GBq ( $\pm 10\%$ ) at the date and time of calibration, according to activity measurements made using a dose calibrator. These data are presented in Figure 2. Out of 100 vials, only 1 patient vial was found to be outside of the manufacturer-specified range.

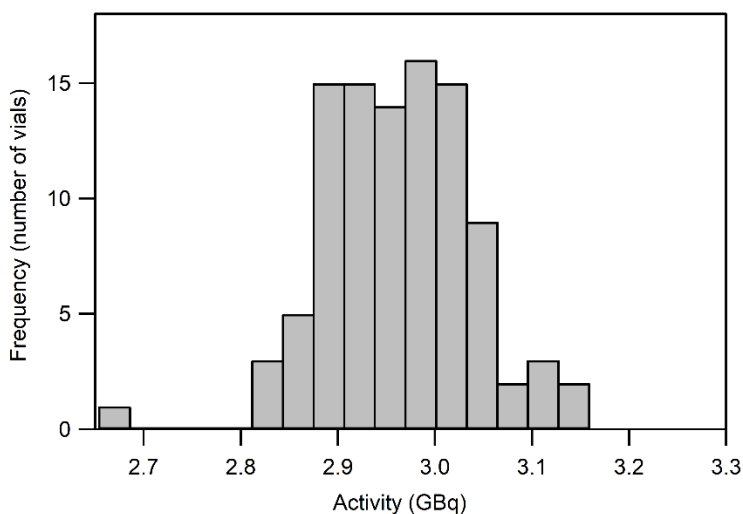


**Figure 2.** Distribution of activities received from the manufacturer at time of calibration, as measured by a manufacturer-traceable dose calibrator. (N=100, received between Feb. 2019 and April 2021).

Activities measured by HPGe assay were found to be substantially higher than manufacturer-specified values. These measurements are summarized in Table 1. The estimated ratio of absolute activity to what has been specified by the manufacturer is  $1.233 \pm 0.030$ . This final value represents the average of results obtained for all samples, and both methods 1 and 2 within each sample.

Activity quantitation by methods 1 & 2 provided virtually identical results, with method 2 yielding values  $\sim 1.0\%$  higher than method 1. Agreement between these methods suggests that the experimentally determined 511 keV detection efficiency (# measured / # emitted) is robust to experimental approach. Background 511 keV count rate ( $0.090 \pm 0.006$  cps) was found to be small in comparison with experimental samples ( $\sim 2.2$  cps). Despite

estimated detector dead times in the range of 22.5 – 25.6%, correction for these effects was found to be accurate when explicitly accounting for a slight bias above ~10% dead time (see Supplemental Material for details).

**Table 1.** Summary of measured patient vial activities, decay corrected to the date and time of calibration.

<b>Sample</b>	<b>Manufacturer (GBq)</b>	<b>HPGe Method 1 (GBq)</b>	<b>HPGe Method 2 (GBq)</b>	<b>HPGe / Manufacturer</b>
1	2.65	3.25 ( $\pm$ 3.8%)	3.28 ( $\pm$ 3.4%)	1.232
2	2.84	3.43 ( $\pm$ 4.2%)	3.46 ( $\pm$ 3.8%)	1.212
3	2.99	3.73 ( $\pm$ 4.0%)	3.77 ( $\pm$ 3.6%)	1.254
4	3.00	3.67 ( $\pm$ 4.0%)	3.71 ( $\pm$ 3.6%)	1.229
5	3.08	3.80 ( $\pm$ 4.2%)	3.83 ( $\pm$ 3.8%)	1.240
			<b>Average:</b>	<b>1.233 <math>\pm</math> 0.030</b>

Variation in the ratio of HPGe-determined activity to dose calibrator-determined activity across samples was consistent with statistical uncertainty within individual measurements. Measurement durations in the range of 3 – 6 hours per patient vial provided statistical uncertainty in measured 511 keV peak areas of 2.5 – 3.1%. Components of overall measurement uncertainty are listed in Table 2, with uncertainty being largely dominated by counting statistical uncertainty (~2.5%), uncertainty in the internal pair production branching ratio of  $^{90}\text{Y}$  (1.48%) (6), efficiency calibration (method 1; 1.9%), and  $^{18}\text{F}$  calibration (method 2; 1.2%). By performing the measurement multiple times, statistical uncertainty was reduced to an acceptable level in the final calibration specification. Uncertainty in the final ratio ( $\pm$  2.47%) includes uncertainty in measurements and systematic effects, having corrected for all known systematic effects.

**Table 2.** Components of measurement uncertainty from a representative patient vial (Sample #1).

Uncertainty	Type A (Method 1 & 2)	Type B (Method 1)	Type B (Method 1 & 2)	Type B (Method 2)
Net peak area	2.50%			
Glass density and thickness (inter-vial variation)			0.40%	
Monte Carlo statistical uncertainty		0.05%		
Glass density and thickness (intra-vial variation)		0.70%		
HDPE density and thickness		0.12%		
Volume and activity-distribution effects		0.50%		0.91%
Efficiency calibration (energy interpolation)		1.50%		
Efficiency calibration (traceable source activities)		1.16%		
Positron range effects (simulated vs. <sup>90</sup> Y)		1.28%		
Dead time correction			0.10%	
Yttrium-90 positron branching ratio			1.48%	
Positron range effects ( <sup>18</sup> F vs. <sup>90</sup> Y)				0.75%
Fluorine-18 activity calibration				1.00%
Fluorine-18 decay correction and residual				0.63%
<b>Total</b>	<b>2.50%</b>	<b>2.45%</b>	<b>1.54%</b>	<b>1.67%</b>
		<b>Average of Method 1 and 2:</b>		<b>3.29%</b>

## DISCUSSION

We have identified a miscalibration associated with the SIR-Spheres<sup>®</sup> product. The ratio of our measured activity levels to those provided by the manufacturer calibration is  $1.233 \pm 0.030$ . This indicates that ~23% more activity has been administered to patients than anticipated and prescribed. Although this result is potentially a regulatory concern (per NRC criteria for reportable medical events,  $\pm 20\%$  from prescribed) *this finding is not immediately concerning from a medical or ethical standpoint.*

From discussion with the manufacturer, this discrepant activity standard has been consistent throughout the availability of this product, including early trials and associated data reviewed by the U.S. Food and Drug Administration for approval (14). This is corroborated by a report in 2008 by R. Selwyn indicating that a SIR-

Spheres<sup>®</sup> vial was found to have  $(26 \pm 1.8)\%$  more activity than the nominal manufacturer value (3.00 GBq  $\pm$  10%) (15). In his measurement, R. Selwyn did not compare directly against the manufacturer activity calibration, however based on our data presented in Figure 2, there is a good chance that the calibrated quantity of activity was between 2.9 – 3.1 GBq, thus implying a miscalibration on the order of 23 – 31%. Additional evidence is presented in a 2007 abstract by S. Moore et al., wherein a calibrated quantity of <sup>90</sup>Y-chloride was utilized to determine appropriate dose calibrator settings for SIR-Spheres. Their reported dose calibrator setting (#24x10, Capintec CRC-15R) was evaluated on the University of Iowa CRC-15R, and it was observed that this dial setting displays ~29% more activity than the manufacturer calibration (#56x10 on our particular device). Work by Ferreira et al. established accurate SIR Sphere calibration factors for the Vinten 671 (0.0678 pA/MBq) and the Capintec CRC-25R (Cal #32x10). Although a CRC-25R was not available for comparison at our institution, use of #32x10 on the University of Iowa CRC-15R displays ~20% more activity than the manufacturer calibration. These reports (15-17), summarized in Table 3, are consistent with our findings and support the theory that a systematic calibration error has been present for SIR-Spheres<sup>®</sup> over the last ~14 years.

**Table 3.** Dose calibrator settings and prior data.

Reference	Dose Calibrator Dial Setting (Model)	Implied Calibration Error
Current SIR Sphere Calibration*	#56x10 (CRC-15R)	-
R. Selwyn, 2008 (15)	-	~23 – 31%
S. Moore, 2007 (16)	#24x10 (CRC-15R)	29%
K. Ferreira, 2016 (17)	#32x10 (CRC-25R)	~20% **
This Work	#29x10 (CRC-15R)	23%

\* Current SIR Sphere Calibration dial setting may differ by institution and instrument, however #56x10 is the setting employed on the University of Iowa CRC-15R to match the manufacturer activity specification.

\*\* Estimated using a CRC-15R, true discrepancy may differ slightly when using the correct model (CRC-25R).

According to the manufacturer, more than 100,000 patients have been treated with SIR-Spheres<sup>®</sup> worldwide, with more than 1,000 healthcare providers currently offering this treatment. This treatment is generally regarded as an excellent option for patients with hepatic tumors. A systematic miscalibration of administered activity has little to no bearing on the accepted safety and efficacy of this agent, however this finding will have significant scientific implications moving forward. Additional efforts by the manufacturer are needed to precisely establish an absolute activity standard for SIR-Spheres<sup>®</sup>. These changes should come about in collaboration with at least one institution capable of making absolute activity measurements, such as NIST or other groups who have already made significant progress toward establishing a SIR-Sphere<sup>®</sup> measurement standard (18,19).

Existing publications addressing liver dose-toxicity relationships with glass and resin microspheres have consistently demonstrated a lower dose toxicity threshold from resin spheres. Work by Chiesa et al. shows that

mean liver doses in excess of 70 Gy from glass microspheres were associated with >50% normal tissue complication probability (NTCP) (20). By comparison, data from resin microspheres indicates that 50% NTCP is associated with a mean liver dose of 52 Gy (95% C.I.: 44 – 61 Gy) (21). With the assumption that prior studies were conducted utilizing manufacturer-recommended activity calibration techniques, the miscalibration identified in our work indicates a somewhat narrower toxicity discrepancy – approximately 64 Gy (resin) vs. 70 Gy (glass) when correcting for this effect. This finding necessitates re-evaluation of published dosimetry data, and interpretations thereof.

The discovery of this miscalibration points to a broader issue in the field of radiopharmaceutical therapy – there is a lack of generalizable methods for independent activity calibration verification by end users, such as what is done in radiation oncology for linear accelerator and sealed source assay. Efforts should be made to extend the capabilities of current accredited dosimetry calibration laboratories to include unsealed sources, or a new mechanism for independent calibration verification should be established.

## **CONCLUSION**

The primary SIR-Spheres® activity calibration appears to be an underestimate of true activity. High-purity germanium spectroscopic measurements of annihilation radiation emissions have provided an estimate of  $1.233 \pm 0.030$  for the ratio of true activity to activity specified by the manufacturer calibration. This finding should be independently verified, and steps should be taken by the manufacturer to establish an accurate and traceable activity standard.

## **ACKNOWLEDGEMENTS**

The authors are grateful for input received from Yusuf Menda and Sandeep Laroia.

## **DISCLOSURE**

The authors have no financial conflicts of interest to disclose. An early version of this manuscript was provided to Sirtex Medical Limited for technical review and comment.

## **KEY POINTS**

**Question:** How do measured SIR Sphere<sup>®</sup> activities compare to the nominal manufacturer calibration?

**Pertinent findings:** The nominal SIR-Spheres<sup>®</sup> activity calibration appears to be an underestimate of true activity. High-purity germanium spectroscopic measurements of annihilation radiation emissions have provided an estimate of  $1.233 \pm 0.030$  for the ratio of true activity to activity specified by the manufacturer calibration.

**Implications for patient care:** A revised activity calibration is needed, which will result in changes to clinical activity prescribing patterns.

## REFERENCES

1. Gleisner KS, Spezi E, Solny P, et al. Variations in the practice of molecular radiotherapy and implementation of dosimetry: results from a European survey. *EJNMMI Phys.* 2017;4:1-20.
2. Mikell J, Cuneo K, Dewaraja Y. Boosting  $^{90}\text{Y}$  SIRT with SBRT: a planning study with  $^{90}\text{Y}$  PET and TCP/NTCP models. Paper presented at: *EJNMMI Res.* 2020.
3. Kasi P, Toskich B, Laroia S. *Immunotherapy with Y90-radioembolization for metastatic colorectal cancer (iRE-C)*. Vol 8: *BMJ Specialist Journals.* 2020.
4. Hobbs RF, McNutt T, Baechler S, et al. A treatment planning method for sequentially combining radiopharmaceutical therapy and external radiation therapy. *Int J Radiat Oncol Biol Phys.* 2011;80:1256-1262.
5. Dietrich A, Koi L, Zöphel K, et al. Improving external beam radiotherapy by combination with internal irradiation. *Br J Radiol.* 2015;88:20150042.
6. Selwyn R, Nickles R, Thomadsen B, DeWerd L, Micka J. A new internal pair production branching ratio of  $^{90}\text{Y}$ : the development of a non-destructive assay for  $^{90}\text{Y}$  and  $^{90}\text{Sr}$ . *Appl Radiat Isot.* 2007;65:318-327.
7. Aarnio P, Nikkinen M, Routti J. SAMPO 90 High resolution interactive gamma-spectrum analysis including automation with macros. *J Radioanal Nucl Chem.* 1992;160:289-295.
8. Zimmerman BE, Cessna JT. Development of a traceable calibration methodology for solid  $^{68}\text{Ge}/^{68}\text{Ga}$  sources used as a calibration surrogate for  $^{18}\text{F}$  in radionuclide activity calibrators. *J Nucl Med.* 2010;51:448-453.
9. Dryak P, Šolc J. Measurement of the branching ratio related to the internal pair production of Y-90. *Appl Radiat Isot.* 2020;156:108942.
10. Chisté V.  $^{90}\text{Y}$ -Comments on evaluation of decay data. *Table of Radionuclides (Comments on evaluation)*.203.
11. Taylor BN, Kuyatt CE. Guidelines for evaluating and expressing the uncertainty of NIST measurement results. *NIST Technical Note 1297.* 1994.
12. ISO I, and BIPM OIML. Guide to the Expression of Uncertainty in Measurement. *Geneva, Switzerland.* 1995;122.
13. Bevington PR, Robinson DK, Blair JM, Mallinckrodt AJ, McKay S. Data reduction and error analysis for the physical sciences. *Computers in Physics.* 1993;7:415-416.
14. Dezarn WA, Cessna JT, DeWerd LA, et al. Recommendations of the American Association of Physicists in Medicine on dosimetry, imaging, and quality assurance procedures for  $^{90}\text{Y}$  microsphere brachytherapy in the treatment of hepatic malignancies. *Med Phys.* 2011;38:4824-4845.
15. Selwyn R, Micka J, DeWerd L, Nickles R, Thomadsen B. The calibration of-labeled SIR-Spheres® using a nondestructive spectroscopic assay. *Med Phys.* 2008;35:1278-1279.
16. Moore S, Park M-A, Limpa-Amara N, Gallagher P, Mahmood A. Measurement of Y-90 resin microsphere activity using dose calibrators. Vol 48 suppl 2: *J Nucl Med;* 2007:74P.

17. Ferreira KM, Fenwick AJ, Arinc A, Johansson LC. Standardisation of  $^{90}\text{Y}$  and determination of calibration factors for  $^{90}\text{Y}$  microspheres (resin) for the NPL secondary ionisation chamber and a Capintec CRC-25R. *Appl Radiat Isot.* 2016;109:226-230.
18. Mo L, Avci B, James D, et al. Development of activity standard for  $^{90}\text{Y}$  microspheres. *Appl Radiat Isot.* 2005;63:193-199.
19. Lourenço V, Bobin C, Chisté V, et al. Primary standardization of SIR-Spheres based on the dissolution of the  $^{90}\text{Y}$ -labeled resin microspheres. *Appl Radiat Isot.* 2015;97:170-176.
20. Chiesa C, Mira M, Maccauro M, et al. A dosimetric treatment planning strategy in radioembolization of hepatocarcinoma with  $^{90}\text{Y}$  glass microspheres. *Q J Nucl Med Mol Imaging.* 2012;56:503-508.
21. Strigari L, Sciuto R, Rea S, et al. Efficacy and toxicity related to treatment of hepatocellular carcinoma with  $^{90}\text{Y}$ -SIR spheres: radiobiologic considerations. *J Nucl Med.* 2010;51:1377-1385.
22. Greenberg JS, Deutsch M. Positrons from the decay of P 32 and Y 90. *Phys Rev.* 1956;102:415.

## SUPPLEMENTAL MATERIAL

### *Monte Carlo methods*

Monte Carlo N-Particle Transport (MCNP) v6.2 and Geant4 Application for Tomographic Emission (GATE) were used for determination of 511 keV self-absorption within the source liquid, vial, and holder. In addition to the primary self-absorption determination, variations in source geometry (e.g. differing glass vial thickness, differing liquid volumes, activity distributed in different portions of the liquid) were simulated to estimate Type B uncertainties in this experiment. Specific values obtained from MCNP were used for all calculations in this work with GATE primarily being utilized as a redundant verification of simulation results. In all geometries tested, GATE and MCNP results agreed within 0.8%. All simulations were performed with  $1 \times 10^{10}$  photon histories, resulting in an overall statistical uncertainty of  $\sim 0.04\%$ .

MCNP simulations were performed by generating isotropic 0.511 MeV photons (PAR = 2, ERG = 0.511) within the source volume, and transport of these photons using default model parameters in MCNP, MODE P. Notable default parameters include 'nocoh=0' (Thomson scattering enabled), 'ispn=0' (photonuclear particle production disabled), 'nodop=0' (Doppler energy broadening enabled), 'CUT:P e=0.001' (Photon cutoff energy = 0.001 MeV). Positron simulations, where applicable (see below), were performed using default model parameters in MCNP, MODE PE. Notable default parameters for electrons/positrons include 'ides=0' (photoelectric, pair and triplet production enabled), 'iphot=0' (Bremsstrahlung production enabled), 'ibad=0' (full Bremsstrahlung tabular angular distribution enabled), and 'istrng=0' (sampling value straggling method used to compute electron energy loss at each collision), 'CUT:E e=0.001' (electron cutoff energy = 0.001 MeV). Within MCNP, positron physics are identical to electron physics, except for positron annihilation. Electrons below the cutoff energy are terminated, whereas positrons below the cutoff energy produce annihilation photons. Primary 511 keV photons reaching the detector (nominally modeled as a 6 cm diameter sphere) were tallied using the MCNP surface current tally (F1), with binning by photon energy ( $>510.9$  keV vs.  $<510.9$  keV). Default model parameters were also used in GATE simulations, with photons reaching the detector being tallied by use of the 'killActor' function with an energy filter of 510.9 – 511.1 keV.

Standard material composition definitions were utilized for water ( $\text{H}_2\text{O}$ ;  $\rho = 1$  g/cm<sup>3</sup>), glass ( $\text{SiO}_2$ ; 2.58 g/cm<sup>3</sup>), high-density polyethylene ( $\text{C}_2\text{H}_4$ ), and air ( $\text{N}_{78}\text{O}_{21}\text{Ar}_1$ ; 1.16 mg/cm<sup>3</sup>). Nominal densities were utilized for all but HDPE, which was directly measured from stock material ( $0.966 \pm 0.009$  g/cm<sup>3</sup>). Microsphere material was assumed to be water-like in all simulations, with decays being randomly generated in the activity volume. Source vial and holder geometries were carefully measured to accurately reproduce source geometry in MCNP and GATE. Glass vial thickness ( $0.224 \pm 0.026$  cm) was determined by deconstructing and measuring the walls of SIR spheres vials. Vials were found to be slightly thicker toward the bottom of the vial, and thinner in the walls ( $\sim 0.18$  cm vs.  $\sim 0.25$  cm). Uncertainties in individual geometric measurements were translated into final 511 keV self-absorption uncertainty by varying various parameters within Monte Carlo simulations (densities, thicknesses,

liquid volume, sphere volume) to determine the effect size of various parameters – see Supplemental Table 1. Self-absorption was found to vary by ~0.8% per mm of HDPE (equivalent to ~10% change in density), by 2.7% per mm of glass (equivalent to ~50% change in density), and by up to ~1% depending on the total volume of liquid in the vial.

Positron range effects were investigated by direct simulation of positron emissions within MCNP, rather than simulation of 511 keV photon primaries. The positron energy spectrum published by Dryák & Šolc(9) indicates an endpoint energy of ~0.75 MeV. MCNP simulations performed with this positron energy (PAR = -3, ERG = 0.75) resulted in a transmission factor of 0.7586 rather than the primary value obtained by simulating 511 keV emissions directly (0.7538). This difference represents a 0.64% increase in transmission. Other literature reports show differences positron energy spectrum however, such as that published by Greenberg and Deutsch,(22) where the endpoint energy appears to be  $\sim 2.4m_0c^2$  (~1.23 MeV). With this uncertainty regarding the Yttrium-90 positron energy spectrum, as well as the relatively small effect size, the decision was made to double the potential transmission difference (1.28%) and include this factor within our Type B uncertainty budget.

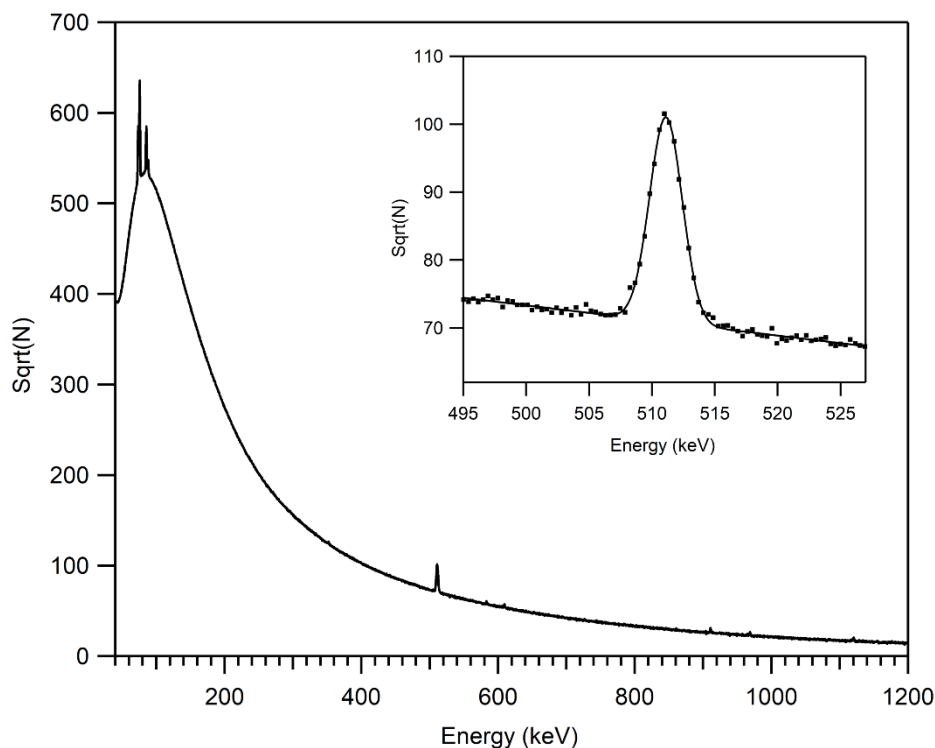
**Supplemental Table 1.** Summary of Monte Carlo results and validation simulations. Transmission values are specified as the ratio of 511 keV emissions reaching HPGe detector with and without self-attenuation. As such, total detection efficiency is the product of transmission, geometric efficiency, and intrinsic efficiency.

Calculation Method	Source Volume	Liquid Volume	Transmission	Parameter Tested
MCNP	3	3	0.772*	Replicate of F-18 source geometry
MCNP	1	5	0.754*	Replicate of SIR Sphere geometry
MCNP	0.5	5	0.738	Volume Effects
MCNP	2	5	0.766	Volume Effects
MCNP	3.5	5	0.772	Volume Effects
MCNP	5	5	0.775	Volume Effects
GATE	5	5	0.782	Volume Effects
MCNP	1	5	0.733	+ 1 mm glass thickness
MCNP	1	5	0.774	- 1 mm glass thickness
MCNP	1	5	0.746	+ 1 mm HDPE
MCNP	1	5	0.774	- 1 mm HDPE
MCNP	1	5	0.759	0.750 MeV positron emissions rather than direct simulation of 0.511 MeV photons
NIST Attenuation Coefficients	-	5	0.781	Point source approximation in center of liquid

\*A transmission value of 0.7538 was utilized for all Method 1 efficiency calculations. For method 2, the ratio of transmission for F-18 to that of Y-90 ( $0.772 / 0.754 = 1.024$ ) was used as a correction factor on apparent detection efficiency determined from NIST-traceable F-18 measurements.

## Gamma Spectra

A representative gamma spectrum is shown in Supplemental Figure 1. As expected, the vast majority of detection events fell within the Bremsstrahlung continuum. A 511 keV peak height to background ratio of ~2 was observed.



**Supplemental Figure 1.** Representative  $^{90}\text{Y}$  gamma spectrum, measured using a high-purity germanium detector.

## Correction for detector dead-time

High-purity germanium detectors are typically operated with <10% dead time due to concerns regarding accurate estimation of live time by the detector system. Detector operation beyond this range requires special consideration.

An experiment was designed to evaluate the accuracy of dead-time estimation for the specific HPGe apparatus utilized in this work. A  $^{137}\text{Cs}$  vial source (calibrated 7.77 MBq on 3/11/1980) was placed at a distance of 80 cm from the detector. With only this source, detector dead time was estimated to be 3.30%. A spectrum was acquired (1000 s live time), and the net 662 keV peak area was measured and corrected for estimated dead time. The result ( $127.34 \pm 0.64$  cps) was taken as a ground-truth measure of  $^{137}\text{Cs}$  detection rate. Following this initial characterization, a second source (~14.8 MBq of  $^{99\text{m}}\text{Tc}$ ) was introduced to the detection geometry, without perturbing the  $^{137}\text{Cs}$  source. Spectra were acquired with the  $^{99\text{m}}\text{Tc}$  source at varying locations, ranging from a

source-to-detector distance of 20 cm to 230 cm. Estimated dead times under these conditions ranged from 6.5% up to 85.1%.

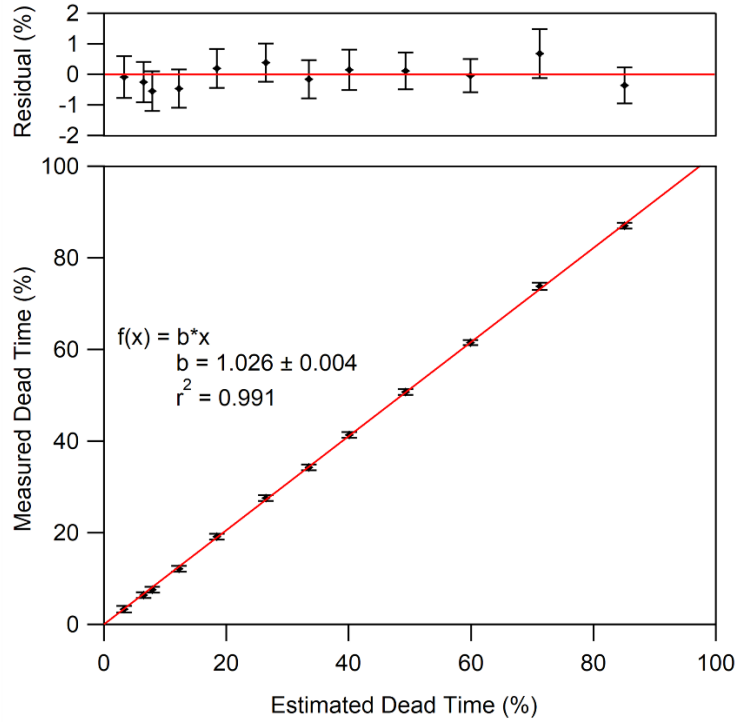
Within the resulting spectra,  $^{137}\text{Cs}$  peak area was assessed, and experimentally measured dead time ( $DT_{meas}$ ) was calculated by

$$DT_{meas} = \frac{R_{meas}}{127.34 \pm 0.64 \text{ cps}}$$

Where  $R_{meas}$  is the measured  $^{137}\text{Cs}$  count rate within an experimental spectrum. Measurement results are listed in Supplemental Table 2. A plot of measured dead time vs. estimated dead time is shown in Supplemental Figure 2. Although generally quite accurate, linear regression reveals a slight bias toward underestimation of true detector dead time. The slope from this regression ( $1.026 \pm 0.004$ ) provides a means to correct for this dead time underestimation in practice. For experimental  $^{90}\text{Y}$  measurements made in this work (22.5 – 25.6% estimated dead time), multiplicative correction factors of 1.0076 – 1.0090 were utilized to correct for dead time estimate inaccuracy.

**Supplemental Table 2.** Ortec dead time estimation in comparison to measured dead time. Measurements are expressed as ( $\mu \pm \sigma$ ).

<b>DT Estimate</b>	<b>DT Measured</b>	<b>Error (Measured - Estimate)</b>	<b>Activity Correction Factor</b>
3.3%	(3.3 ± 0.7) %	0.0%	1.001
6.5%	(6.4 ± 0.7) %	-0.1%	1.002
7.9%	(7.6 ± 0.7) %	-0.3%	1.002
12.3%	(12.1 ± 0.6) %	-0.2%	1.004
18.5%	(19.1 ± 0.6) %	0.7%	1.006
26.5%	(27.5 ± 0.6) %	1.1%	1.009
33.5%	(34.2 ± 0.7) %	0.7%	1.013
40.1%	(41.3 ± 0.7) %	1.2%	1.018
49.3%	(50.7 ± 0.6) %	1.4%	1.026
59.9%	(61.4 ± 0.5) %	1.5%	1.040
71.2%	(73.7 ± 0.8) %	2.5%	1.069
85.1%	(86.9 ± 0.6)%	1.8%	1.174



**Supplemental Figure 2.** Plot of measured dead time vs. Ortec estimated dead time. Constraining  $f(0) = 0$  (assumption of accurate dead-time estimation at low count rates), linear regression reveals a slope of  $1.026 \pm 0.004$ .

### *Correction for radioactive decay during counting*

Decay correction during spectral acquisition was performed by standard methods. With the assumption that dead time does not change significantly during acquisition, the number of counts acquired ( $N$ ) can be expressed as:

$$N = \int_0^{T_{real}} \frac{T_{live}}{T_{real}} I_0 e^{-\lambda t} dt$$

Where  $T_{real}$  and  $T_{live}$  are the acquisition real- and live-time, respectively,  $I_0$  is the incidence rate at  $t=0$ , and  $\lambda$  is the radioactive decay constant. Evaluating this integral and solving for  $I_0$  yields the following:

$$I_0 = \left( \frac{N}{T_{live}} \right) \left( \frac{\lambda T_{real}}{1 - e^{-\lambda T_{real}}} \right)$$

In this formula,  $N/T_{live}$  is the decay-corrected detection rate, and the second term,  $\lambda T_{real} / (1 - e^{-\lambda T_{real}})$ , corrects for decay during spectral acquisition.

### ***Correction for radionuclide impurities***

No radionuclide impurities were detected in the samples measured as a part of this work. Previous works have suggested Yttrium-88 as a notable impurity, which would have required consideration if detected due to the positron decay branch of  $^{88}\text{Y}$ .

### ***Correction for differing $^{18}\text{F}$ and $^{90}\text{Y}$ source geometries***

Pursuant to HPGe efficiency calibration (method 2), the impact of differing source geometry between  $^{18}\text{F}$  and  $^{90}\text{Y}$  measurements was characterized. During measurements  $^{18}\text{F}$  was uniformly distributed in 3 mL within the SIR Sphere vial and source holder, whereas the SIR Spheres were evenly distributed within the bottom ~1 mL of the vial, with ~5 mL of total volume. These source geometries were modeled within MCNP 6.2, and the difference in efficiency for 511 keV detection was found to be  $2.36\% \pm 0.05\%$ . This correction was utilized for all HPGe (method 2) results.

### ***Correction for Bremsstrahlung-induced pair production***

MCNP 6.2 simulations were performed to estimate the prevalence of Bremsstrahlung-induced external pair production within the source container and surrounding structures. Approximately 31 pair production events were observed per billion  $^{90}\text{Y}$  decays, for an estimated probability of  $0.031 \times 10^{-6}$  per decay. In comparison to the internal pair production branching ratio of  $^{90}\text{Y}$  ( $(31.86 \pm 0.47) \times 10^{-6}$ ), this phenomenon constitutes an effect size of ~0.10%. This effect size was deemed to be well within overall measurement uncertainty and was thus omitted from analysis.